

Self-dual compact gauged baby skyrmions in a continuous medium

C. A. I. Florián,^{*} Rodolfo Casana,[†] and André C. Santos[‡]

Departamento de Física, Universidade Federal do Maranhão, 65080-805, São Luís, Maranhão, Brazil.

We investigate the existence of self-dual configurations in the restricted gauged baby Skyrme model enlarged with a \mathbb{Z}_2 -symmetry, which introduces a real scalar field. For such a purpose, we implement the Bogomol'nyi procedure that provides a lower bound for the energy and the respective self-dual equations whose solutions saturate such a bound. Aiming to solve the self-dual equations, we specifically focused on a class of topological structures called compacton. We obtain the corresponding numerical solutions within two distinct scenarios, each defined by a scalar field, allowing us to describe different magnetic media. Finally, we analyze how the compacton profiles change when immersed in each medium.

I. INTRODUCTION

The Skyrme model [1] is a (3+1)-dimensional nonlinear field theory conceived initially to study some nonperturbative aspects of quantum Chromodynamics (QCD); for example, it provides physical properties of hadrons and nuclei [2] compatible with the low-energy regimen of QCD. The hadrons described by the Skyrme model emerge as topological solitons, so-called skyrmions. The (2+1)-dimensional or planar version [3], known as the baby Skyrme model, is a laboratory to study many aspects of the original Skyrme model. Like the original version, the baby Skyrme model consists of a $O(3)$ nonlinear sigma term, the Skyrme one, and a nonlinear potential, $V(\hat{n} \cdot \vec{\phi})$, stabilizing the solitons [4]. The Skyrme field $\vec{\phi}$ is a unit three-component vector of scalar fields $\vec{\phi} = (\phi_1, \phi_2, \phi_3)$ obeying $\vec{\phi} \cdot \vec{\phi} = 1$, so describing the unit sphere \mathbb{S}^2 . The unitary vector \hat{n} gives a preferential direction in the internal space \mathbb{S}^2 [5]. The Skyrme model is invariant under the $SO(3)$ symmetry, while the potential partially breaks this symmetry, keeping the $SO(2)$ symmetry unchanged (which is isomorphic to the $U(1)$ one). Further, the potential must satisfy the condition $V(\phi_n) \rightarrow 0$ when $\phi_n \rightarrow 1$, known as the single vacuum configuration. Although the baby Skyrme model describes stable solitons, it does not support a Bogomol'nyi-Prasad-Sommerfield (BPS) structure [6], i.e., an energy lower-bound (the Bogomol'nyi bound) and a set of self-dual equations providing solitons that saturate this energy bound. On the other hand, in the absence of the sigma term arises the so-called restricted baby Skyrme model [7], which supports BPS or self-dual configurations [8].

A natural physical extension for the Skyrme model is to couple it with a $U(1)$ gauge field [9], which allows us to investigate the electric and magnetic properties. In this context, Ref. [10] provides the first study showing that the restricted gauge baby Skyrme model supports a BPS structure. Afterward, BPS or self-dual solutions carrying both magnetic flux and electric charge were obtained [11–13]. Such studies in the restricted gauge baby Skyrme model have shown different BPS soliton profiles, i.e., it supports compact and noncompact topological structures. Concerning the compact skyrmions, Ref. [7] provides the first investigation checking their existence into the restricted baby Skyrme model (nongauged version). Further, studies considering the sigma term as $\epsilon \partial_\mu \vec{\phi} \cdot \partial^\mu \vec{\phi}$ [14, 15] show that such a model in the limit $\epsilon \rightarrow 0$ reproduces exactly the BPS structure of the restricted baby Skyrme model obtained in the Ref. [8]. Posteriorly, studies of the gauged version revealed that it also engenders compactons [16] endowed with magnetic flux, but electrically neutral [10]. Moreover, recently, compactons carrying both the magnetic flux and electric charge were also found [12]. Regarding the restricted gauged baby Skyrme model, its BPS structure is related to the $N = 2$ SUSY gauged Skyrme model in (2+1)-dimensions, whose bosonic Lagrangian requires the disappearance of the term $D_\mu \vec{\phi} \cdot D^\mu \vec{\phi}$, as established in Refs. [17].

It is well-known that gauge models can be enlarged or extended by including a new symmetry, for example, in the Maxwell-Higgs model [18]. Within that context, new topological defects by adding a \mathbb{Z}_2 -symmetry recently have been founded in the Maxwell-Higgs models [19, 20], magnetic monopoles [21], gauged $CP(2)$ model [22], and gauged $O(3)$ sigma model [23]. Remarkably, this additional symmetry can engender a magnetic or dielectric medium that could profoundly affect the solitons' physical properties.

On the other hand, the so-called magnetic skyrmions have attracted the community's attention because they come up in the description of various physical systems as, e.g., in condensed matter [24], in the quantum Hall effect [25], superconductors [26], and magnetic materials [27], including recent investigations with the Dzyaloshinskii-Moriya

^{*} cesar.aif@discente.ufma.br

[†] rodolfo.casana@ufma.br; rodolfo.casana@gmail.com

[‡] andre.cs@discente.ufma.br; andre_cavs@hotmail.com

(DM) interaction [28, 29]. Furthermore, in the condensed matter context, effects induced on the topological structures due to geometrical constraints in the magnetic materials at the nanometric scale are reported, i.e., the geometry's influence on the formation of magnetic skyrmions [30–33], there are also among them those with compact support that are very sensitive to geometrical constraints [34–37].

Taking the ideas discussed in the previously, we seek new topological configurations in limited planar regions simulating geometrical restrictions. For this purpose, we introduce an extended version of the gauged BPS baby Skyrme model to study solitonic solutions, focusing on compactons immersed in a magnetic medium [38]. Thus, the original symmetry $SO(3)$ is enlarged to $SO(3) \times \mathbb{Z}_2$, being the \mathbb{Z}_2 -symmetry that rules a neutral scalar field coupled to the Abelian gauge field through a magnetic permeability that is a function of the scalar field itself. Consequently, in our case, including the \mathbb{Z}_2 -symmetry allows us to modify the compacton profiles, whereas we keep them in geometrically constrained regions.

We present the results in the following way: In Sec. II, we introduce our model and show the corresponding Euler-Lagrange equations. Besides, we found the BPS structure of the system and solved the respective BPS equations by considering rotationally symmetric configurations. In Sec. III, we study two scenarios describing different magnetic media and solve the BPS system numerically; then, we highlight the new features presented by the new compacton profiles. Lastly, we make our final remarks and conclusions in Sec. IV.

II. THE RESTRICTED GAUGED BABY SKYRME MODEL IN A MAGNETIC MEDIUM

We investigate an extension of the restricted baby Skyrme model immersed in a magnetic medium driven by a real scalar field defined by the Lagrangian

$$L = E_0 \int d^2 \mathbf{x} \mathcal{L}, \quad (1)$$

where E_0 is a common factor that sets the energy scale (which hereafter we will take as $E_0 = 1$) and \mathcal{L} is the Lagrangian density [39] given by

$$\mathcal{L} = -\frac{1}{4g^2} \Sigma(\chi) F_{\mu\nu} F^{\mu\nu} - \frac{\lambda^2}{4} (D_\mu \vec{\phi} \times D_\nu \vec{\phi})^2 + \frac{1}{2} \partial_\mu \chi \partial^\mu \chi - V(\phi_n, \chi), \quad (2)$$

with the non-negative real function $\Sigma(\chi)$ setting the electromagnetic properties of the medium as a function of the real scalar field χ introduced to incorporate the \mathbb{Z}_2 -symmetry. $F_{\mu\nu} = \partial_\mu A_\nu - \partial_\nu A_\mu$ is the strength-tensor of the Abelian gauge field A_μ , g is the electromagnetic coupling constant, and λ the Skyrme coupling constant. In addition, the Skyrme and gauge fields are coupled minimally through the covariant derivative

$$D_\mu \vec{\phi} = \partial_\mu \vec{\phi} + A_\mu \hat{n} \times \vec{\phi}. \quad (3)$$

The potential $V(\phi_n, \chi)$ stands for some appropriated interaction in terms of both the Skyrme and the scalar fields. Furthermore, the scalar fields $\vec{\phi}$ and χ are dimensionless, the gauge field and the electromagnetic coupling constant g possess mass dimension 1, and the Skyrme coupling constant λ has mass dimension -1 .

It is important to emphasize that the system is at vacuum when $\Sigma(\chi) = 1$, indicating that the field χ decouples from the gauge field, reducing (2) to the gauged BPS baby Skyrme model investigated in Ref. [10].

The Euler-Lagrange equations obtained from the Lagrangian density (2) are

$$\partial_\mu (\Sigma F^{\mu\nu}) = g^2 j^\nu, \quad (4)$$

$$D_\mu \vec{J}^\mu + \frac{\partial V}{\partial \phi_n} \hat{n} \times \vec{\phi} = 0, \quad (5)$$

$$\partial_\mu \partial^\mu \chi + \frac{1}{4} \Sigma_\chi F_{\mu\nu} F^{\mu\nu} + V_\chi = 0, \quad (6)$$

where $\Sigma_\chi = \partial \Sigma / \partial \chi$, $V_\chi = \partial V / \partial \chi$ and $j^\mu = \hat{n} \cdot \vec{J}^\mu$ is the conserved current density with

$$\vec{J}^\mu = \lambda^2 [\vec{\phi} \cdot (D^\mu \vec{\phi} \times D^\nu \vec{\phi})] D_\nu \vec{\phi}. \quad (7)$$

In the present study, we are interested in stationary soliton solutions of the model described by the Lagrangian density (2). In this sense, from Eq. (4), we extract an important information via the stationary Gauss law

$$\partial_i(\Sigma\partial_i A_0) = g^2\lambda^2 A_0(\hat{n} \cdot \partial_i \vec{\phi})^2, \quad (8)$$

which is identically satisfied by gauge condition $A_0 = 0$, allowing us to choose such a condition henceforth. Consequently, the system solutions only carry on magnetic flux. Furthermore, from Eq. (4), we also obtain the stationary Ampère law, which is given by,

$$\partial_i(\Sigma B) + g^2\lambda^2(\hat{n} \cdot \partial_i \vec{\phi})Q = 0, \quad (9)$$

where $B = F_{12} = \epsilon_{ij}\partial_i A_j$ is the magnetic field and Q is

$$Q = \vec{\phi} \cdot (D_1 \vec{\phi} \times D_2 \vec{\phi}) = q + \epsilon_{ij} A_i(\hat{n} \cdot \partial_j \vec{\phi}). \quad (10)$$

The quantity q related to the topological charge density of the Skyrme field is given by

$$q = \frac{1}{2}\epsilon_{ij}\vec{\phi} \cdot (\partial_i \vec{\phi} \times \partial_j \vec{\phi}), \quad (11)$$

such that the topological charge or topological degree (or winding number) of the Skyrme field reads as

$$\text{deg}[\vec{\phi}] = -\frac{1}{4\pi} \int q d^2\mathbf{x} = k, \quad (12)$$

where $k \in \mathbb{Z} \setminus 0$.

The stationary equation for the Skyrme field obtained from Eq. (5) reads

$$D_k \vec{J}_k - \frac{\partial V}{\partial \phi_n} \hat{n} \times \vec{\phi} = 0, \quad (13)$$

whereas, from Eq. (6), we obtain for the χ -field

$$\partial_k \partial_k \chi - \frac{1}{2} \Sigma_\chi B^2 - V_\chi = 0. \quad (14)$$

In the next section, we implement the Bogomol'nyi procedure [6] to investigate the conditions under which the model (2) engenders self-dual or BPS configurations that minimize the energy of the system.

A. The BPS structure

The starting point is the stationary energy density of the model defined by the Lagrangian density (2), which reads as

$$\varepsilon = \frac{1}{2g^2} \Sigma B^2 + \frac{\lambda^2}{2} Q^2 + \frac{1}{2} (\partial_k \chi)^2 + V(\phi_n, \chi), \quad (15)$$

where we have used the gauge condition $A_0 = 0$. In order to ensure a finite energy, the following boundary conditions must be satisfied:

$$\lim_{|\mathbf{x}| \rightarrow \infty} \sqrt{\Sigma} B = 0, \quad \lim_{|\mathbf{x}| \rightarrow \infty} Q = 0, \quad \lim_{|\mathbf{x}| \rightarrow \infty} \partial_k \chi = 0, \quad \lim_{|\mathbf{x}| \rightarrow \infty} V(\phi_n, \chi) = 0. \quad (16)$$

In what follow, the total de energy reads

$$E = \int \left[\frac{1}{2g^2} \Sigma B^2 + \frac{\lambda^2}{2} Q^2 + \frac{1}{2} (\partial_k \chi)^2 + V \right] d^2\mathbf{x}, \quad (17)$$

and to implement the Bogomol'nyi procedure, we introduce three auxiliary functions, $W \equiv W(\phi_n)$, $Z \equiv Z(\phi_n)$ and the functions $F_i \equiv F_i(\chi)$ (with $i = 1, 2$), that allows us to express total energy as

$$E = \int \left[\frac{(\Sigma B \pm g^2 \lambda^2 W)^2}{2g^2 \Sigma} + \frac{1}{2} \left(\partial_k \chi \mp \epsilon_{kj} \frac{\partial F_j}{\partial \chi} \right)^2 + \frac{\lambda^2}{2} (Q \mp Z)^2 \mp \lambda^2 B W \pm \lambda^2 Q Z \pm \epsilon_{kj} \partial_k F_j + V - \frac{g^2 \lambda^4 W^2}{2 \Sigma} - \frac{\lambda^2}{2} Z^2 - \frac{1}{2} \left(\frac{\partial F_j}{\partial \chi} \right)^2 \right] d^2\mathbf{x}. \quad (18)$$

Now, by setting

$$Z = \frac{\partial W}{\partial \phi_n}, \quad (19)$$

and using Eq. (10), the expression $\mp \lambda^2 B W \pm \lambda^2 Q Z$ becomes

$$\pm \lambda^2 \epsilon_{ij} \partial_j (A_i W) \pm \lambda^2 q \left(\frac{\partial W}{\partial \phi_n} \right), \quad (20)$$

with q defined in Eq. (11). Further, by setting

$$V = \frac{g^2 \lambda^4 W^2}{2 \Sigma} + \frac{\lambda^2}{2} \left(\frac{\partial W}{\partial \phi_n} \right)^2 + \frac{1}{2} \left(\frac{\partial F_j}{\partial \chi} \right)^2, \quad (21)$$

we establish a relation between the potential and the respective superpotentials. Next, the vacuum condition in Eq. (16), allows us to establish

$$\lim_{|\mathbf{x}| \rightarrow \infty} W = 0, \quad \lim_{|\mathbf{x}| \rightarrow \infty} \frac{\partial W}{\partial \phi_n} = 0, \quad \lim_{|\mathbf{x}| \rightarrow \infty} \frac{\partial F_j}{\partial \chi} = 0, \quad (22)$$

by considering Σ^{-1} a well-behaved function. Here it is interesting to point out that both $W(\phi_n)$ and $F_i(\chi)$ play the role of superpotential functions, the first one for the Skyrme field ϕ and the second for the scalar field χ . The choosing of both the superpotentials must consider that the resultant self-dual potential (21) ensures the finite-energy requirement, i.e., the energy density (15) must be null when the fields attain their vacuum values.

The first condition in (22) tell us the integral of the total derivative $\epsilon_{ij} \partial_j (A_i W)$ is zero, i.e.,

$$\int \epsilon_{ij} \partial_j (A_i W) d^2 \mathbf{x} = 0. \quad (23)$$

This way, the considerations so far allow us to write Eq. (18) as

$$E = E_{\text{BPS}} + \frac{1}{2g^2} \int \frac{(\Sigma B \pm g^2 \lambda^2 W)^2}{\Sigma} d^2 \mathbf{x} + \frac{\lambda^2}{2} \int \left(Q \mp \frac{\partial W}{\partial \phi_n} \right)^2 d^2 \mathbf{x} + \frac{1}{2} \int \left(\partial_k \chi \mp \epsilon_{kj} \frac{\partial F_j}{\partial \chi} \right)^2 d^2 \mathbf{x}, \quad (24)$$

with E_{BPS} defined by

$$E_{\text{BPS}} = \int \left[\pm \lambda^2 q \left(\frac{\partial W}{\partial \phi_n} \right) \pm \epsilon_{kj} (\partial_k F_j) \right] d^2 \mathbf{x} > 0, \quad (25)$$

where the first term is the Skyrmion contribution to the BPS energy and the second stands for the additional contribution coming from the χ -field sector.

The total energy satisfy the inequality $E \geq E_{\text{BPS}}$, attaining its minimum $E = E_{\text{BPS}}$ when the Bogomol'nyi bound is saturated, i.e., the fields satisfying the following set of equations:

$$\Sigma B = \mp g^2 \lambda^2 W, \quad (26)$$

$$Q = \pm \frac{\partial W}{\partial \phi_n}, \quad (27)$$

$$\partial_k \chi = \pm \epsilon_{kj} \frac{\partial F_j}{\partial \chi}. \quad (28)$$

The set above defines the self-dual or BPS equations of the model (2). The solutions of these BPS equations can also be considered classical solutions belonging to an extended supersymmetric model [40, 41] whose bosonic sector would be given by the Lagrangian density (2). Some studies concerning skyrmions in the SUSY field theory context, including compactons, can be found, for example, in Refs. [15, 17, 42] for nongauged models and in Ref. [43] for the gauged ones.

Lastly, we highlight that the presence of the neutral scalar field χ in our model (2) demands the insertion of the superpotentials $F_i(\chi)$ to complete its BPS structure. Below, the superpotentials $F_i(\chi)$ will be chosen to generate suitable solutions in the scalar sector to define the magnetic permeability $\Sigma(\chi)$.

B. BPS Skyrmions with radial symmetry

We now consider rotationally symmetric solitons and also we set, without loss of generality, $\hat{n} = (0, 0, 1)$ such that $\phi_n = \phi_3$. The standard ansatz for the Skyrme field is

$$\vec{\phi}(r, \theta) = \begin{pmatrix} \sin f(r) \cos(N\theta) \\ \sin f(r) \sin(N\theta) \\ \cos f(r) \end{pmatrix}, \quad (29)$$

where r and θ are polar coordinates, $N = \text{deg}[\vec{\phi}]$ is the winding number presented in Eq. (12), and $f(r)$ is a well behaved function obeying the boundary conditions

$$f(0) = \pi, \quad \lim_{r \rightarrow \infty} f(r) = 0. \quad (30)$$

By convenience, we introduce the following field redefinition [10]:

$$\cos f(r) = 1 - 2h(r), \quad (31)$$

with the field $h(r)$ obeying

$$h(0) = 1, \quad \lim_{r \rightarrow \infty} h(r) = 0. \quad (32)$$

Further, for the gauge field components and neutral scalar field we assume

$$A_i = -\epsilon_{ij} x_j \frac{Na(r)}{r^2}, \quad \chi = \chi(r), \quad (33)$$

respectively. The fields $a(r)$ and $\chi(r)$ are regular functions satisfying, at the origin, the conditions

$$a(0) = 0, \quad \chi(0) = \chi_0, \quad (34)$$

whereas for the asymptotic limit we require

$$\lim_{r \rightarrow \infty} a(r) = a_\infty, \quad \lim_{r \rightarrow \infty} \chi(r) = \chi_\infty, \quad (35)$$

where χ_0 , χ_∞ and a_∞ are finite constants.

The magnetic flux is easily calculated to be

$$\Phi = 2\pi \int_0^R Br dr = 2\pi Na(R) = 2\pi Na_R, \quad (36)$$

where $a_R = a(R)$ is a real constant, whereas $R > 0$ defines the maximum size of the configuration characterizing the type of solution, i.e., R is finite for compact solutions and infinite for noncompact solutions (see, e.g., Refs. [10, 12, 44]). As well as their counterpart model [10], the magnetic flux (36) is nonquantized since a_R and a_∞ (when $R \rightarrow \infty$) belong to the interval $\langle -1, 0 \rangle$. It is a characteristic property of Skyrme models that for sufficiently large values of the electromagnetic coupling g , the quantities a_R or a_∞ tend to -1 and, in such a limit, the magnetic flux becomes “quantized” in units of 2π .

For the radial superpotentials, we take

$$W \equiv W(h(r)), \quad (37)$$

and

$$F_i = -\epsilon_{ij} x_j \frac{\mathcal{W}(\chi(r))}{r^2}. \quad (38)$$

For convenience, we write the radial version of the BPS potential (21) as the sum of two contributions

$$V = V^{(\Sigma)} + V^{(\chi)}, \quad (39)$$

where

$$V^{(\Sigma)} = \frac{g^2 \lambda^4}{2} \frac{W^2}{\Sigma} + \frac{\lambda^2}{8} W_h^2, \quad V^{(\chi)} = \frac{1}{2r^2} \mathcal{W}_\chi^2, \quad (40)$$

being $W_h = \partial W / \partial h$ and $\mathcal{W}_\chi = \partial \mathcal{W} / \partial \chi$. The vacuum condition for the potential $V(h, \chi)$ provides the boundary conditions for W and W_h as set in Eq. (22), whereas for the \mathcal{W}_χ we have

$$\lim_{r \rightarrow \infty} \mathcal{W}_\chi = 0. \quad (41)$$

Further, the superpotentials $W(h)$ and $\mathcal{W}(\chi)$ are regular functions obeying the following boundary conditions at the origin:

$$W(h(0)) = W(1) = W_0, \quad (42)$$

$$\mathcal{W}(\chi(0)) = \mathcal{W}(\chi_0) = \mathcal{W}_0, \quad (43)$$

whereas for the asymptotic limit we get

$$\lim_{r \rightarrow \infty} W(h) = W(0) = 0, \quad (44)$$

$$\lim_{r \rightarrow \infty} \mathcal{W}(\chi) = \mathcal{W}(\chi_\infty) = \mathcal{W}_\infty, \quad (45)$$

where W_0 , \mathcal{W}_0 and \mathcal{W}_∞ are constants, and they are in accordance with the boundary conditions (32), (34) and (35).

We observe in the BPS potential (39) the contribution $V^{(\chi)}$, which, per the proposal in (38), becomes out to be an explicit function of the radial coordinate. Nevertheless, we emphasize that such explicit dependence in the radial coordinate allows circumventing [45] the Derrick-Hobard scaling theorem [4]. Consequently, it allows us to attain stable kinklike solutions in the χ -field sector, as previously considered in literature in different scenarios [19–23].

Let us now show the BPS energy density under radial symmetry which, as well as BPS potential (39), is interesting to be expressed as the sum of two contributions

$$\varepsilon_{\text{BPS}} = \varepsilon_\Sigma + \varepsilon_\chi, \quad (46)$$

where we have defined

$$\varepsilon_\Sigma = \frac{g^2 \lambda^4}{\Sigma} W^2 + \frac{\lambda^2}{4} W_h^2 \quad \text{and} \quad \varepsilon_\chi = \frac{\mathcal{W}_\chi^2}{r^2}, \quad (47)$$

respectively. The quantity ε_Σ represents the energy density associated purely with the new skyrmion configurations, while ε_χ is the contribution associated with the kinklike solution engendered by scalar field χ .

The energy's lower bound (or Bogomol'nyi bound) in Eq. (25) becomes

$$E_{\text{BPS}} = \pm 2\pi (\lambda^2 N W_0 + \Delta \mathcal{W}) > 0, \quad (48)$$

where the integration has been performed using the boundary conditions (42), (43), (44), and (45). Furthermore, we have defined the quantity $\Delta \mathcal{W} = \mathcal{W}_\infty - \mathcal{W}_0$, such that the upper (lower) sign in (48) describes the self-dual solitons (antisolitons) corresponding to N and $\Delta \mathcal{W}$ positive (negative) quantities.

The set of BPS equations (26), (27) and (28), reads

$$B = \frac{N}{r} \frac{da}{dr} = \mp g^2 \lambda^2 \frac{W}{\Sigma}, \quad (49)$$

$$Q = \frac{2N}{r} (1+a) \frac{dh}{dr} = \mp \frac{W_h}{2}, \quad (50)$$

$$\frac{d\chi}{dr} = \pm \frac{\mathcal{W}_\chi}{r}, \quad (51)$$

respectively. We now observe that the third BPS equation (51) has no explicit dependence on the functions $h(r)$ and $a(r)$, allowing it to be solved separately by adequately choosing the superpotential $\mathcal{W}(\chi)$. The kinklike solution obtained from Eq.(51) defines the magnetic permeability $\Sigma(\chi)$ appearing explicitly in the BPS equation (49). Consequently, once $\Sigma(\chi)$ is known, we proceed to solve the two self-dual equations (49) and (50).

At this level, to define the model entirely, we observe that it is necessary to choose the functions $W(h)$ and $\mathcal{W}(\chi)$. Thus, for our analysis, we may consider functions $W(h)$ already studied in other BPS Skyrme models (see, e.g., Refs. [10, 12, 13, 44]). For the function $\mathcal{W}(\chi)$ associated with the neutral scalar field χ , we will consider the ones engendering kinklike solutions. Furthermore, such as in other Skyrme's models [10, 12, 44], we have verified that the our BPS model here studied support compact and noncompact skyrmions. Namely, by taking a given superpotential $W(h)$, the type of skyrmion engendered is determined by analyzing how the fields approach their respective vacuum values. For such a purpose, it is considered a superpotential $W(h)$ whose behavior is

$$W(h) \approx W_R^{(\sigma)} h^\sigma, \quad (52)$$

near the vacuum, where $W_R^{(\sigma)} > 0$ and $\sigma > 1$. Thus, the analysis is performed by taking now the boundary conditions

$$h(r) = 0, \quad a(r) = a_R, \quad W(h(r)) = 0, \quad (53)$$

being R and a_R are quantities already introduced in (36). The σ values characterize the soliton solutions. Indeed, for $1 < \sigma < 2$, we have the soliton called compacton, whose vacuum value is reached in a finite radius R (the compacton's radius) and remains in the vacuum for all $r > R$, see e.g. Refs. [12, 44]. Otherwise, for $\sigma \geq 2$ we have the radius $R \rightarrow \infty$ which provides extended or noncompact configurations that result in localized or delocalized solitons, see e.g. Refs. [12, 13, 44].

In the remainder of the manuscript, we only study solitonic solutions by adopting the upper sign, i.e., $N > 0$ and $\Delta\mathcal{W} > 0$. Specifically, our principal focus is to analyze compact skyrmion's new properties that could appear when immersed in a magnetic medium.

III. BPS SKYRMIONS IN MAGNETIC MEDIA: COMPACTONS

To investigate BPS compactons, we choose the superpotential as being

$$W(h) = W_0 h^{3/2}, \quad (54)$$

where W_0 is a constant. An important detail is that this superpotential provides a potential $V^{(\Sigma)} \propto h$ when $r \rightarrow R$, this being analogous to the so-called "old baby Skyrme potential" [10].

The next step is to specify some functional form for both the superpotential $\mathcal{W}(\chi)$ and the magnetic permeability $\Sigma(\chi)$. For such a goal, we will consider two superpotentials (that engendering the χ^4 and χ^6 models, respectively) supplying kinklike solitons that we use to define the magnetic permeability appearing in the BPS equation (49). This way, it will be possible to analyze how the magnetic medium modifies the shape of the compact BPS skyrmions.

A. χ^4 medium

In our first scenario, we consider a superpotential $\mathcal{W}(\chi)$ engendering a χ^4 model, i.e.,

$$\mathcal{W}(\chi) = \alpha\chi - \frac{\alpha}{3}\chi^3, \quad (55)$$

where α is a nonnegative real parameter. In the literature, we find this superpotential applied in different contexts, for example, in the study of vortices with internal structures [19, 20, 22, 23], magnetic monopoles [21], skyrmion-like configurations [46, 47], and the behavior of massless Dirac fermions in a skyrmion-like background [48]. Then, by using (55) in (51) and solving the BPS equation, we obtain the exact kinklike solution

$$\chi(r) = \frac{r^{2\alpha} - r_0^{2\alpha}}{r^{2\alpha} + r_0^{2\alpha}}, \quad (56)$$

with r_0 being an arbitrary positive constant such that $\chi(r_0) = 0$. This solution satisfies the boundary conditions $\chi(0) = \chi_0 = -1$ and $\chi(\infty) = \chi_\infty = 1$. In this case, the BPS bound (48) for the energy becomes

$$E_{\text{BPS}} = 2\pi\lambda^2 N W_0 + \frac{8}{3}\alpha\pi, \quad (57)$$

where the last term is the contribution from the neutral scalar field χ .

We must now select the function defining the magnetic permeability of the medium where the compact skyrmions will stay immersed. For this, we have inspired ourselves with investigations regarding the pattern formation of ringlike solitons [49, 50] in a two-dimensional Bose-Einstein condensate interacting with a harmonic oscillator, which provides periodic modulation to the system. Our approach will adjust the magnetic permeability using a periodic function to modulate the topological structures. This way, we set it as

$$\Sigma(\chi) = \frac{1}{\sin^2(m\pi\chi)}, \quad (58)$$

where $m \in \mathbb{N}$. Further, functions like that also has been used, for example, in the study of kinklike solutions [51] and vortexlike structures [20, 23].

This way, the energy density ε_Σ results be

$$\varepsilon_\Sigma = g^2 \lambda^4 W_0^2 h^3 \sin^2(m\pi\chi) + \frac{9}{16} \lambda^2 W_0^2 h. \quad (59)$$

Already the BPS equations (49) and (50) to be investigated assume the form

$$\frac{N}{r}(1+a) \frac{dh}{dr} + \frac{3}{8} W_0 h^{1/2} = 0, \quad (60)$$

$$\frac{N}{r} \frac{da}{dr} + g^2 \lambda^2 W_0 \sin^2 \left(m\pi \frac{r^{2\alpha} - r_0^{2\alpha}}{r^{2\alpha} + r_0^{2\alpha}} \right) h^{3/2} = 0, \quad (61)$$

which we must solve with suitable field boundary conditions to provide compact skyrmions in the current scenario.

Before we solve the BPS equations numerically, let us show the behavior of the field profiles close to the boundary values. Thus, near to the origin, by taking the more relevant terms, the Skyrme and gauge field profiles behave as,

$$h(r) = 1 - \frac{3}{2^4} \frac{W_0}{N} r^2 + \frac{3^2}{2^{10}} \frac{W_0^2}{N^2} r^4 - \frac{3}{2^4} \frac{C_0 W_0}{(\alpha+1)(2\alpha+1)N^2} \frac{r^{4\alpha+4}}{r_0^{4\alpha}} + \dots, \quad (62)$$

$$a(r) = -\frac{2C_0}{(2\alpha+1)N} \frac{r^{4\alpha+2}}{r_0^{4\alpha}} + \frac{3^2}{2^5} \frac{C_0 W_0}{(\alpha+1)N^2} \frac{r^{4\alpha+4}}{r_0^{4\alpha}} + \frac{4C_0}{(3\alpha+1)N} \frac{r^{6\alpha+2}}{r_0^{6\alpha}} + \dots, \quad (63)$$

where we have defined the constant $C_0 = \pi^2 m^2 g^2 \lambda^2 W_0$. In the sequel, we present the behavior, close to the origin, of both the magnetic field and the energy density $\varepsilon_\Sigma(r)$. Then, the magnetic field reads

$$B(r) = -4C_0 \frac{r^{4\alpha}}{r_0^{4\alpha}} + \frac{3^2}{2^3} \frac{C_0 W_0}{N} \frac{r^{4\alpha+2}}{r_0^{4\alpha}} - \frac{3^3}{2^8} \frac{C_0 W_0^2}{N^3} \frac{r^{4\alpha+4}}{r_0^{4\alpha}} + 8C_0 \frac{r^{6\alpha}}{r_0^{6\alpha}} + \dots, \quad (64)$$

showing that it is null in $r = 0$, whereas the energy density $\varepsilon_\Sigma(r)$ reading as

$$\varepsilon_\Sigma = \frac{3^2}{2^4} \frac{\lambda^2 W_0^2}{N} - \frac{3^3}{2^8} \frac{\lambda^2 W_0^3}{N} r^2 + \frac{3^4}{2^{14}} \frac{\lambda^2 W_0^4}{N^2} r^4 + 4C_0 \lambda^2 W_0 \frac{r^{4\alpha}}{r_0^{4\alpha}} + \dots, \quad (65)$$

presents a nonnull value at the origin.

On the other hand, near the vacuum values, i.e., when $r \rightarrow R$, the field profiles possess the following behavior:

$$h(r) \approx \frac{3^2}{2^8} \frac{R^2 W_0^2}{(1+a_R)^2 N^2} (r-R)^2, \quad (66)$$

$$a(r) \approx a_R + \frac{1}{2^2} \frac{R^2}{N^2} C_R (r-R)^4, \quad (67)$$

with the constant C_R defined as

$$C_R = \frac{3^3}{2^{12}} \frac{g^2 \lambda^2 W_0^4 R^2}{(1+a_R)^3 N^2} \sin^2 \left(m\pi \frac{R^{2\alpha} - r_0^{2\alpha}}{R^{2\alpha} + r_0^{2\alpha}} \right), \quad (68)$$

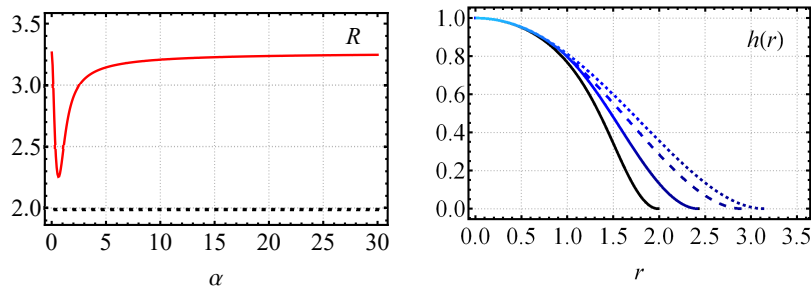


FIG. 1. Depiction by assuming the magnetic permeability (58) with $r_0 = 0.5$, $m = 1$ and distinct values for α . Left: compacton radius R vs. α (solid red line) and the compacton radius of the standard case (black dot line). Right: the present Skyrme field (color lines) is depicted for $\alpha = 1$ (solid line), $\alpha = 2$ (dashed line) and $\alpha = 5$ (dot line), and the solid black line represents the profile without the magnetic medium.

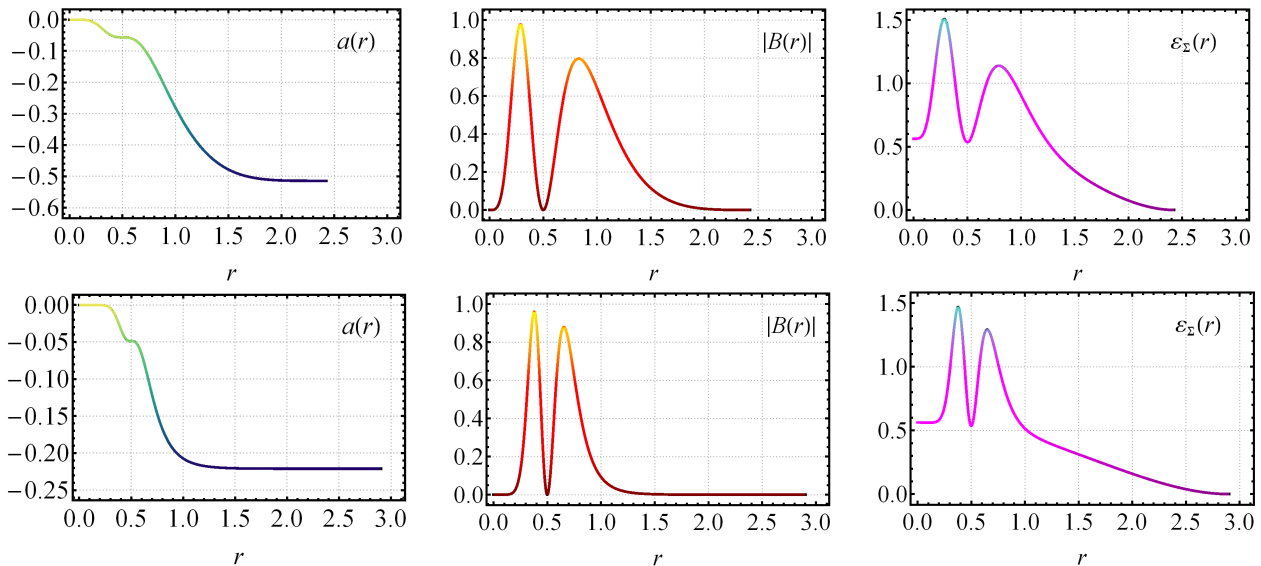


FIG. 2. The gauge field profiles $a(r)$ (left panels), absolute value of the magnetic field $|B(r)|$ (middle panels) and energy density $\varepsilon_\Sigma(r)$ (right panels). We depict for $r_0 = 0.5$, $m = 1$ with $\alpha = 1$ (top) and $\alpha = 2$ (bottom).

which depends on the new parameters m , α and r_0 that control the medium. Similarly, the first relevant terms of the magnetic field and energy density ε_Σ , when $r \rightarrow R$, are given by

$$B(r) = -\frac{R}{N}C_R(r-R)^3 + \dots, \quad (69)$$

and

$$\begin{aligned} \varepsilon_\Sigma = & \frac{3^4}{2^{12}} \frac{\lambda^2 W_0^4 R^2}{(1+a_R)^2 N^2} (r-R)^2 + \dots \\ & + \frac{3^3}{2^{12}} \frac{\lambda^2 W_0^4 R^4}{(1+a_R)^3 N^4} C_R (r-R)^6 + \dots \end{aligned} \quad (70)$$

We next solve the BPS system, Eqs. (61) and (60), numerically to investigate how the magnetic permeability (58) modifies the soliton profiles. For such a purpose, we fix $N = 1$, $W_0 = 1$, $\lambda = 1$, $g = 1$, by considering distinct values of both α and m , besides, r_0 will have a specified value in each case. It is important to point out that although the fixed parameters also could be explored (e.g., by running different values), we have used only α and m to control the profile shape of the fields. Both parameters are enough to exhibit the main features of the compact skyrmions immersed in the medium defined by (58).

We have begun our analysis by investigating how the compacton radius R changes as a function of the α parameter for a fixed r_0 and m , shown in the left panel of Fig. 1. Likewise, we have verified that exists an interval $0 < \alpha \leq \bar{\alpha}$

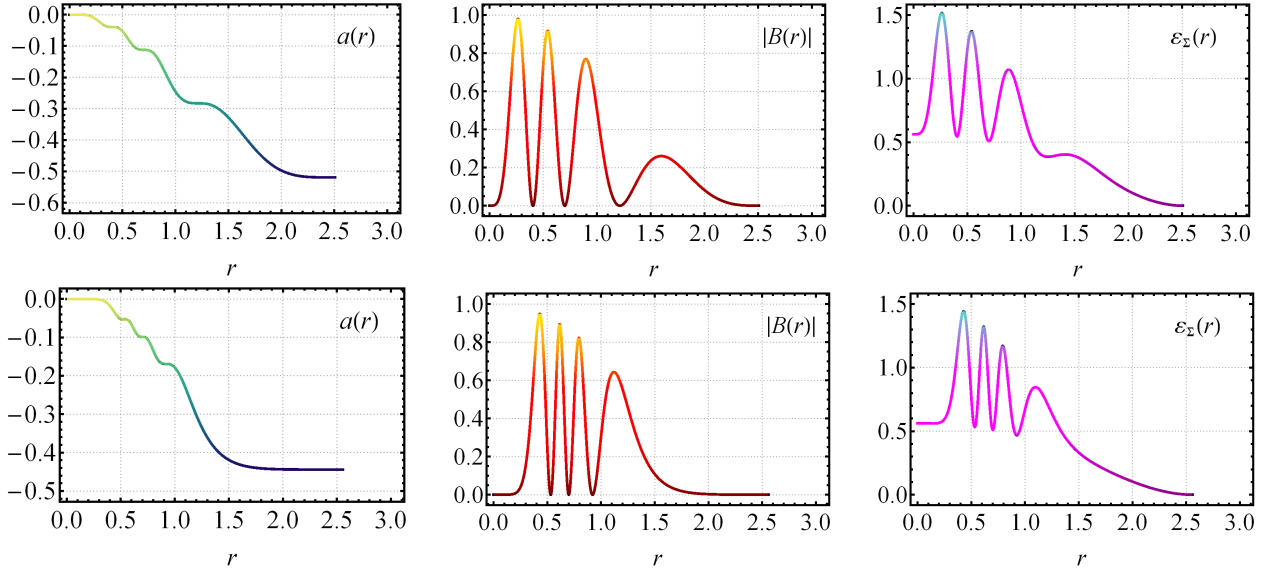


FIG. 3. The gauge field profiles $a(r)$ (left panels), absolute value of the magnetic field $|B(r)|$ (middle panels) and energy density $\varepsilon_\Sigma(r)$ (right panels). We depict for $r_0 = 0.7$, $m = 2$ with $\alpha = 1$ (top) and $\alpha = 2$ (bottom).

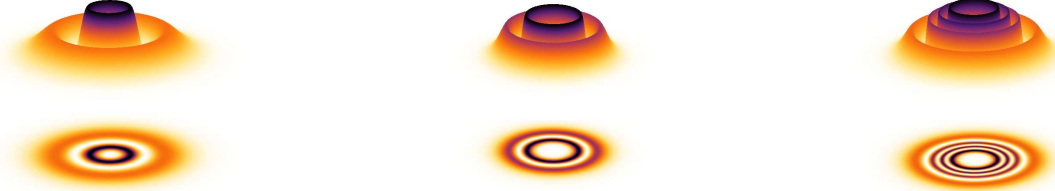


FIG. 4. The magnetic field distributions (upper plots) with their corresponding projections in the plane (bottom plots). We depict for $r_0 = 0.7$ with $m = 1$ and $\alpha = 1$ (left plot), $m = 1$ and $\alpha = 2$ (middle plot), and $m = 2$ and $\alpha = 2$ (right plot).

(here $\bar{\alpha} \simeq 0.6$) that provides global extreme values for the compacton radius. Namely, for a sufficiently small α (close to zero) we have the maximum compacton radius $R_{\max} \simeq 3.26$ which decreases until it reaches the minimum value $R_{\min} \simeq 2.25$ when $\alpha = \bar{\alpha}$. From this point on, i.e., for $\alpha > \bar{\alpha}$, the values of R begins to increase in a way that $R \rightarrow R_{\max}$. We also observe that the magnetic medium modifies the compacton radius, which achieves higher values than the ones acquired without the medium (we will call $R_0 \simeq 1.99$, see the horizontal black dotted line). Alike, in the right panel of Fig. 1, we illustrate this effect on the Skyrme field profiles by depicting $h(r)$ for some values of $\alpha > \bar{\alpha}$. So, we observe how the parameter α modifies the profiles by showing the increase of the compacton radius as α grows.

Figure 2 shows the profiles for the gauge field $a(r)$, magnetic field $B(r)$ and energy density $\varepsilon_\Sigma(r)$, all of them well-behaved functions and in according to the respective behaviors previously found at the boundary values. The gauge field $a(r)$ profiles acquire a plateau format around r_0 that affect directly the profiles of both the magnetic field and $\varepsilon_\Sigma(r)$, i.e., because of the plateau, they acquire a ringlike shape centered at the origin. We also note that when α increases, the profiles become more localized around r_0 . On the other hand, the role played by the parameter m is better understood by examining Fig. 3. We have verified that for a fixed m , the gauge field engenders $(2m - 1)$ -plateaus that define, in the profiles of both $B(r)$ and $\varepsilon_\Sigma(r)$, an equal number of outer rings around its center. For a more precise overview of these features, we depict in Fig. 4 the effects induced in the magnetic field profiles by the magnetic permeability (58) for different values of α and m . It is notorious how α controls the magnetic field distribution around the origin. That is, the size of the inner region to the ringlike structures increases as α grows; that effect arises because the rings agglomerate around r_0 when α growths (see left and middle plots in Fig. 4). In addition, we see the explicit formation of $2m - 1$ outer rings, corresponding to the same quantity of plateaus engendered in the gauge profile.

Therefore, our results show how the magnetic permeability (58), induced by the kinklike soliton of the χ^4 -model, provides new features to the profiles of both the magnetic field and the BPS energy density of the compact skyrmions originally at the vacuum, i.e., when $\Sigma(\chi) = 1$.

B. χ^6 medium

In this second scenario, we adopt a superpotential that engenders a χ^6 model, so we consider

$$\mathcal{W}(\chi) = \frac{\alpha}{2}\chi^2 - \frac{\alpha}{4}\chi^4, \quad (71)$$

which has also been used in the study of multilayered structures [20]. Then, by using (71) in the BPS equation (51), we obtain the kinklike solution generated by the χ^6 -model that is given by

$$\chi(r) = \frac{r^\alpha}{\sqrt{r^{2\alpha} + r_0^{2\alpha}}}, \quad (72)$$

satisfying the following boundary values $\chi_0 = 0$ and $\chi_\infty = 1$. Likewise, now the BPS bound (48) becomes

$$E_{\text{BPS}} = 2\pi\lambda^2 N W_0 + \frac{\alpha\pi}{2}, \quad (73)$$

where the second term is the contribution from the neutral scalar field χ .

To investigate the changes in the shape of the soliton originate from a χ^6 model, we select the following magnetic permeability,

$$\Sigma(\chi) = \frac{1}{J_0^2(\gamma\chi)}, \quad (74)$$

where J_0 is the zero-order Bessel function of the first kind and $\gamma \in \mathbb{R}$. The primary motivation for this choice is the ringlike patterns that solitons produce in Bessel photonic lattices when interacting with a nonlinear medium, as mentioned in Refs. [52, 53]. These studies specifically investigated the behavior of optical radiation in a bulk cubic medium subjected to a transverse modulation of the linear refractive index. Our current study will observe that the magnetic permeability (74) plays a modulation role, contributing to the raising of compact skyrmions with ring-shaped structures, too.

Taking $\Sigma(\chi)$ defined in (74), the BPS equations to be solved are given by to the ones in (60) and the second equation now reads

$$\frac{N}{r} \frac{da}{dr} + g^2 \lambda^2 W_0 J_0^2 \left(\frac{\gamma r^\alpha}{\sqrt{r^{2\alpha} + r_0^{2\alpha}}} \right) h^{3/2} = 0. \quad (75)$$

It is also important to write the energy density $\varepsilon_\Sigma(r)$ for the current scenario,

$$\varepsilon_\Sigma = g^2 \lambda^4 W_0^2 h^3 J_0^2 + \frac{9}{16} \lambda^2 W_0^2 h. \quad (76)$$

To continue, we write below the behavior of the field profiles near the boundary values. Like this, around the origin, we obtain

$$\begin{aligned} h(r) &= 1 - \frac{3}{2^4} \frac{W_0}{N} r^2 + \frac{3}{2^{10}} \frac{(16g^2\lambda^2 - 3) W_0^2}{N^2} r^4 + \dots \\ &+ \frac{3}{2^6} \frac{\gamma^2 g^2 \lambda^2 W_0^2}{(\alpha + 1)(\alpha + 2) N^2} \frac{r^{2\alpha+4}}{r_0^{2\alpha}} + \dots, \end{aligned} \quad (77)$$

$$\begin{aligned} a(r) &= -\frac{\lambda^2 g^2 W_0}{2N} r^2 + \frac{3^2 g^2 \lambda^2 W_0^2}{2^7 N^2} r^4 + \dots \\ &+ \frac{\gamma^2 g^2 \lambda^2 W_0}{4N(1 + \alpha)} \frac{r^{2\alpha+2}}{r_0^{2\alpha}} + \dots. \end{aligned} \quad (78)$$

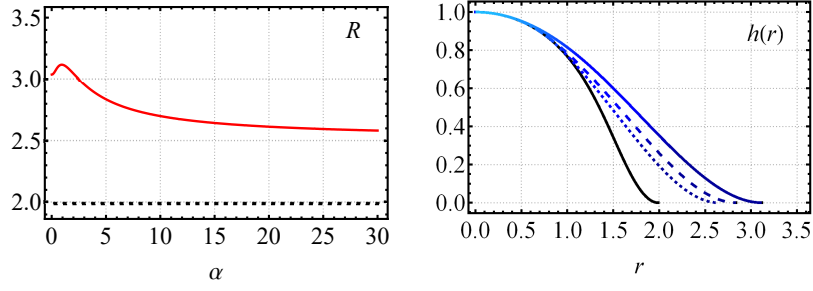


FIG. 5. Depiction by assuming the magnetic permeability (74) with $\gamma = 6$ and distinct values for α . Left: compacton radius R vs. α (solid red line) and the compacton radius of the standard case (black dot line). Right: the present Skyrme field (color lines) is depicted for $\alpha = 1$ (solid line), $\alpha = 5$ (dashed line), and $\alpha = 15$ (dot line), and the solid black line represents the profile at the vacuum ($\Sigma(\chi) = 1$).

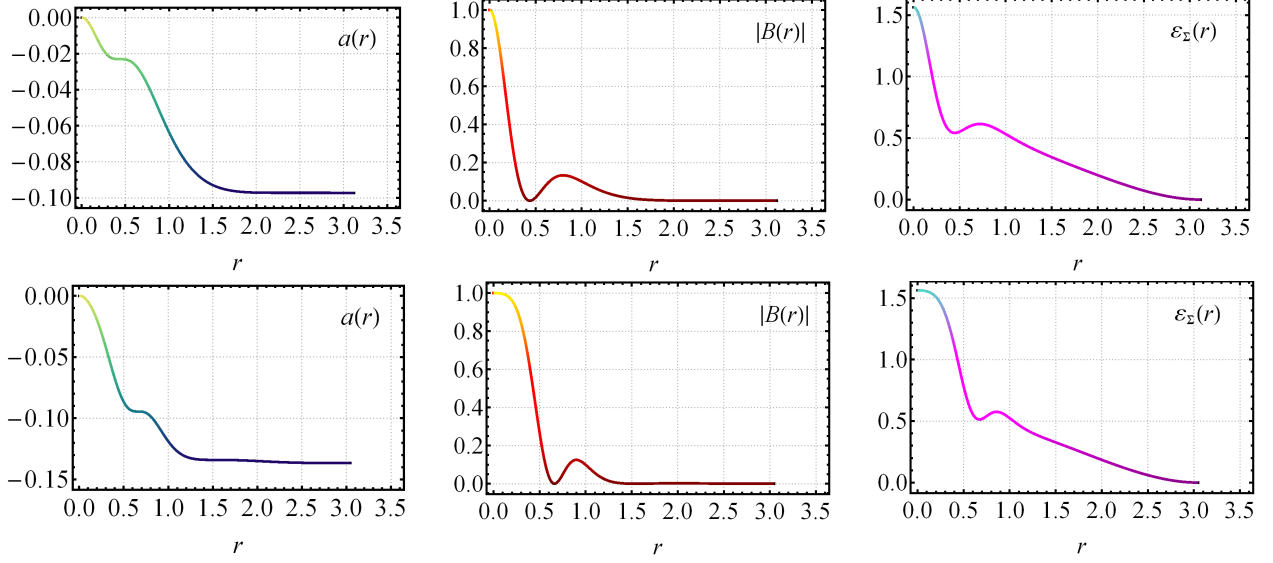


FIG. 6. The gauge field profiles $a(r)$ (left panels), absolute value of the magnetic field $|B(r)|$ (middle panels) and energy density $\varepsilon_\Sigma(r)$ (right panels). We depict for $\gamma = 6$ with $\alpha = 1$ (top) and $\alpha = 2$ (bottom).

Besides, for the magnetic field and the energy density ε_Σ we get

$$B(r) \approx -\lambda^2 g^2 W_0 + \frac{3^2 g^2 \lambda^2 W_0^2}{2^5 N} r^2 + \dots + \frac{\gamma^2 g^2 \lambda^2 W_0}{2} \frac{r^{2\alpha}}{r_0^{2\alpha}} + \dots, \quad (79)$$

and

$$\varepsilon_\Sigma = g^2 \lambda^4 W_0^2 + \frac{3^2}{2^4} \lambda^2 W_0^2 - \frac{3^2 \lambda^2 (16g^2 \lambda^2 + 3) W_0^3}{2^8 N} r^2 + \dots - \frac{\gamma^2 g^2 \lambda^4 W_0^2}{2} \frac{r^{2\alpha}}{r_0^{2\alpha}} + \dots, \quad (80)$$

respectively. Moreover, we observe that both are nonnull at the origin.

The field profiles in the limit $r \rightarrow R$, i.e., when they reach the corresponding vacuum value, possess the following behavior:

$$h(r) \approx \frac{3^2}{2^8} \frac{W_0^2 R^2}{(1 + a_R)^2 N^2} (r - R)^2 + \dots \quad (81)$$

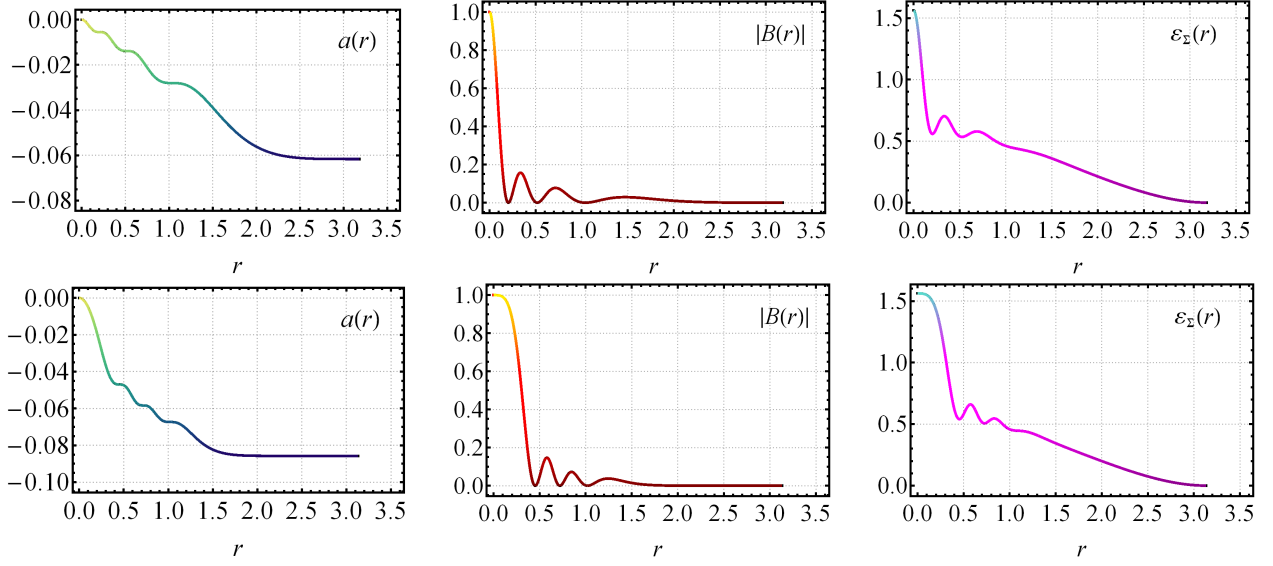


FIG. 7. The gauge field profiles $a(r)$ (left panels), absolute value of the magnetic field $|B(r)|$ (middle panels) and energy density $\varepsilon_{\Sigma}(r)$ (right panels). We depict for $\gamma = 12$ with $\alpha = 1$ (top) and $\alpha = 2$ (bottom).

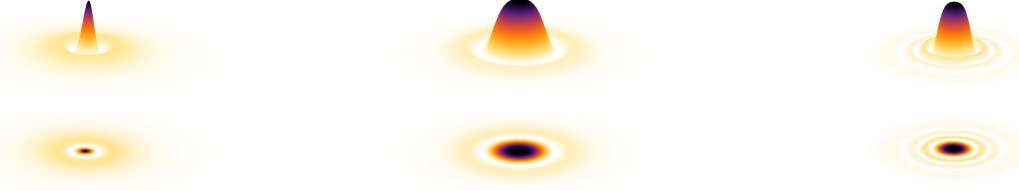


FIG. 8. The magnetic field distributions (upper plots) with their corresponding projections in the plane (bottom plots). We depict for $r_0 = 0.7$ with $\gamma = 6$ and $\alpha = 1$ (left plot), $\gamma = 6$ and $\alpha = 2$ (middle plot), and $\gamma = 12$ and $\alpha = 2$ (right plot).

$$a(r) \approx a_R + \frac{1}{2^2} \frac{g^2 R^2}{(1+a_R) N^2} \mathcal{C}_R (r-R)^4 + \dots, \quad (82)$$

where \mathcal{C}_R is a constant given by

$$\mathcal{C}_R = \frac{3^3}{2^{12}} \frac{\lambda^2 W_0^4 R^2}{(1+a_R)^2 N^2} J_0^2 \left(\frac{\gamma R^\alpha}{\sqrt{R^{2\alpha} + r_0^{2\alpha}}} \right), \quad (83)$$

depending on the parameters γ , α and r_0 that control the medium. Furthermore, the first relevant terms contributing to both the magnetic field and energy density ε_{Σ} in the limit $r \rightarrow R$ are

$$B(r) = -\frac{g^2 R}{(1+a_R) N} \mathcal{C}_R (r-R)^3 + \dots \quad (84)$$

and

$$\begin{aligned} \varepsilon_{\Sigma} = & \frac{3^4}{2^{12}} \frac{\lambda^2 W_0^4 R^2}{(1+a_R)^2 N^2} (r-R)^2 + \dots \\ & + \frac{3^3}{2^{12}} \frac{g^2 \lambda^2 W_0^4 R^4}{(1+a_R)^4 N^4} \mathcal{C}_R (r-R)^6 + \dots \end{aligned} \quad (85)$$

We next present the numerical solutions for the fields by solving the system of BPS equations (60) and (75). Again we have fixing $N = 1$, $W_0 = 1$, $\lambda = 1$, $g = 1$ and $r_0 = 1$ (when adopted other value will be shown), for different values of α and m .

To analyze how the compacton radius R changes, we depict R vs. α (see left panel of Fig. 5). We remark the existence of an interval $0 < \alpha \leq \bar{\alpha}$ (here $\bar{\alpha} \simeq 0.9$) where the compacton radius grows until to reach a maximum value $R_{\max} \simeq 3.12$ when $\alpha = \bar{\alpha}$, a behavior unlike from the previous case. Thereafter, for $\alpha > \bar{\alpha}$, the values of the radius monotonically decrease tending asymptotically to a minimum value $R \rightarrow R_{\min}$ (here, $R_{\min} \simeq 2.51$). This effect is illustrated in the right panel of Fig. 5 where it is depicted $h(r)$ for some values of $\alpha > \bar{\alpha}$. The picture shows how the profiles are modified, while the compacton radius decreases as α grows.

In Figs. 6 and 7 we have depicted the profiles for the gauge field $a(r)$, magnetic field $B(r)$ and energy density $\varepsilon_{\Sigma}(r)$. They behave according to the analytical expressions calculated previously at the boundaries. We also observe plateaus arising along the gauge field profiles; the inner plateau that shapes the core becomes bigger while α grows. Consequently, the presence of the plateaus engenders ringlike structures in the profiles of both the $B(r)$ and $\varepsilon_{\Sigma}(r)$. Thus, in Fig. 8, we highlight the new effects in the magnetic field profiles: first, one notices that α controls the core size, whose radius increases as α grows (see left and middle plots). Second, the parameter γ controls the number of outer rings (surrounding the respective soliton's core) that increase while γ grows.

IV. CONCLUSIONS

We have shown that BPS skyrmions also arise in an enlarged restricted gauged baby Skyrme model with $SO(3) \times \mathbb{Z}_2$ -symmetry. The \mathbb{Z}_2 -symmetry introduces a neutral field χ that includes nonlinearities also engendering solitonic structures. The interaction between both the gauge and scalar fields happens through the magnetic permeability $\Sigma(\chi)$, i.e., via the coupling $\Sigma(\chi)F_{\mu\nu}F^{\mu\nu}$. The successful implementation of the BPS procedure allows for obtaining the Bogomol'nyi bound and the corresponding self-dual equations whose solutions saturate such a bound.

We have verified that the extended gauged baby Skyrme model proposed here also engenders compact and non-compact topological structures. However, the manuscript focuses on compact skyrmions by studying how they are affected by including the \mathbb{Z}_2 -symmetry guiding the functional form of the magnetic permeability $\Sigma(\chi)$. Then, to define the magnetic permeability, we investigated two scenarios characterized by the superpotentials engendering the χ^4 and χ^6 models, respectively. Henceforth, the effects on the compactons immersed in those media were analyzed separately. Both analyses reveal that the \mathbb{Z}_2 -symmetry alters the profiles of the solitons. Among the features induced by the \mathbb{Z}_2 -symmetry, we list: (i) it changes the compacton radius size; (ii) it promotes the arising of the ringlike format, and (iii) it controls the inner region size and the number of outer rings surrounding the center.

We know the physical differences between the skyrmions studied here [38] and the magnetic skyrmions researched in condensed matter, including those obtained considering the DM interaction. Both cases possess finite energy topological configurations, which include compactons. Then, a natural question arises about the possibility of a unified description by investigating whether both interactions could coexist to engender novel solutions. Indeed, in a recent study reported in Ref. [54], the authors introduce the DM interaction in the baby Skyrme model through the effective potential technique, even obtaining compact skyrmions. This approach may pave the way to understanding the connection between the skyrmion studied here and the magnetic skyrmions arising in condensed matter. Still in this direction, it could be possible to initiate the study concerning the BPS structure of the baby Skyrme model in the presence of the DM interaction.

Finally, already we have some issues under consideration, including the baby Skyrme model in the presence of the DM interaction, as the engendering of compact skyrmions (carrying only magnetic flux and the ones with both magnetic flux and electrically charged) in the presence of magnetic media, magnetic impurities, and other topological (nontopological) objects. Advances in these directions we will report elsewhere.

ACKNOWLEDGMENTS

This study was financed in part by the Coordenação de Aperfeiçoamento de Pessoal de Nível Superior - Brasil (CAPES) - Finance Code 001. We thank also the Conselho Nacional de Desenvolvimento Científico e Tecnológico (CNPq), and the Fundação de Amparo à Pesquisa e ao Desenvolvimento Científico e Tecnológico do Maranhão (FAPEMA) (Brazilian Government agencies). R. C. acknowledges the support from the grants CNPq/306724/2019-7, FAPEMA/Universal-01131/17, FAPEMA/Universal-00812/19, and FAPEMA/APP-12299/22. In particular, A. C. S. thank the grants CAPES/88882.315461/2019-01 and CNPq/150402/2023-6 and C. A. I. F. thanks the support from

-
- [1] T.H.R. Skyrme, Proc. R. London **260**, 127 (1961); Nucl. Phys. **31** 556 (1962); J. Math. Phys. (N. Y.) **12**, 1735 (1971).
- [2] G.S. Adkins, C.R. Nappi, and E. Witten, Nucl. Phys. **B228** 552 (1983); G.S. Adkins and C.R. Nappi, Nucl.Phys. **B233** 109 (1984); C.J. Halcrow, C. King, and N.S. Manton, Phys. Rev. C **95**, 031303(R) (2017); C. Naya and P. Sutcliffe, Phys. Rev. Lett. **A983**, 276 (2019).
- [3] B. M. A. G. Piette, B. J. Schroers, and W. J. Zakrzewski, Z. Phys. C **65**, 165 (1995); Nucl. Phys. **B439**, 205 (1995).
- [4] R. H. Hobart, Proc. Phys. Soc. London **82**, 201 (1963); G. H. Derrick, J. Math. Phys. (N.Y.) **5**, 1252 (1964).
- [5] We use this notation for the Skyrme field and the unitary vector along the manuscript; besides, the quantity $\hat{n} \cdot \vec{\phi}$ will be denoted as ϕ_n .
- [6] E. Bogomol'nyi, Sov. J. Nucl. Phys. **24**, 449 (1976). M. Prasad and C. Sommerfield, Phys. Rev. Lett. **35**, 760 (1975).
- [7] T. Gisiger and M.B. Paranjape, Phys. Rev. D **55**, 7731 (1997).
- [8] C. Adam, T. Romanczukiewicz, J. Sanchez-Guillen, and A. Wereszczynski, Phys. Rev. D **81**, 085007 (2010).
- [9] E. Witten, Nucl. Phys. B223, 422 (1983); B223, 433 (1983); C. G. Callan and E. Witten, Nucl. Phys. B239, 161 (1984).
- [10] C. Adam, C. Naya, J. Sanchez-Guillen, and A. Wereszczynski. Phys. Rev. D **86**, 045010 (2012).
- [11] C. Adam, C. Naya, J. Sanchez-Guillen, and A. Wereszczynski, J. High Energy Phys. 03 (2013) 012.
- [12] Rodolfo Casana, André C. Santos, Claudio F. Farias, and Alessandro L. Mota, Phys. Rev. D **100**, 045022 (2019).
- [13] Rodolfo Casana, André C. Santos, Claudio F. Farias, and Alessandro L. Mota, Phys. Rev. D **101**, 045018 (2020).
- [14] S. B. Gudnason, M. Barsanti, S. Bolognesi, JHEP 11(2020)062; JHEP05(2021)134.
- [15] S. Bolognesi and W. Zakrzewski, Phys. Rev. D 91, 045034 (2015).
- [16] C. Adam, P. Klimas, J. Sanchez-Guillen, and A. Wereszczynski. Phys. Rev. D **80**, 105013 (2009).
- [17] C. Adam, J. M. Queiruga, J. Sanchez-Guillen, A. Wereszczynski, J. High Energy Phys. 05 (2013) 108; J. M. Queiruga, J. Phys. A **52**, 055202 (2019).
- [18] E. Witten, Nucl. Phys. B249, 557 (1985); A. J. Peterson, M. Shifman, and G. Tallarita, Ann. Phys. (Amsterdam) 353, 48 (2015).
- [19] D. Bazeia, M. A. Marques, and R. Menezes, Phys. Lett. B **780**, 485 (2018).
- [20] D. Bazeia, M. A. Liao, M. A. Marques, and R. Menezes, Phys. Rev. Research **1**, 033053 (2019).
- [21] D. Bazeia, M. A. Marques, and R. Menezes, Phys. Rev. D **97**, 105024 (2018).
- [22] J. Andrade, R. Casana, E. da Hora, and C. dos Santos. Phys. Rev.D **99**, 056014, (2019).
- [23] R. Casana, André C. Santos, and M. L. Dias, Phys. Rev. D **102**, 085002 (2020).
- [24] G.E. Volovik, *Exotic Properties of Superfluid ^3He* (World Scientific, Singapore, 1992); *The Universe in Helium Droplet* (Oxford University Press, New York, 2009).
- [25] S.L. Sondhi, A. Karlhede, S.A. Kivelson, and E.H. Rezayi, Phys. Rev. B **47**, 16419 (1993); O. Schwindt and N.R.Walet, Europhys. Lett. **55**, 633 (2001); A.C. Balram, U. Wursbauer, A. Wojs, A. Pinczuk, and J.K. Jain, Nat. Commun. **6**, 8981 (2015); T. Chen and T. Byrnes, Phys. Rev. B **99**, 184427 (2019).
- [26] A.A. Zyuzin, J.Garaud, and E. Babaev, Phys. Rev. Lett. **119**, 167001 (2017); S. M. Dahir, A. F. Volkov, and I.M. Eremin Phys. Rev. Lett. **122**, 097001 (2019).
- [27] S. Mühlbauer, B. Binz, F. Jonietz, C. Pfleiderer, A. Rosch, A. Neubauer, R. Georgii, and P. Boni, Science **323**, 915 (2009); X.Z. Yu, Y. Onose, N. Nagaosa, and Y. Tokura, Nature (London) **465**, 901 (2010); T. Dohi, S. DuttaGupta, S. Fukami, and H. Ohno, Nat. Commun. **10**, 5153 (2019).
- [28] T. Dohi, S. DuttaGupta, S. Fukami, and H. Ohno, Nat. Commun. **10**, 5153 (2019).
- [29] B. J. Schroers, SciPost Phys. **7**, 030 (2019); B. Barton- Singer, C. Ross, and B. J. Schroers, Commun. Math. Phys. **375**, 2259 (2020).
- [30] Y. Zhou and M. Ezawa, Nat. Commun. **5**, 4652 (2014).
- [31] W. Jiang, P. Upadhyaya, W. Zhang, G. Yu, M. B. Jungesch, F. Y. Fradin, J. E. Pearson, Y. Tserkovnyak, K. L. Wang, O. Heinonen, S. G. E. te Velthuis, and A. Homann, Science **349**, 283 (2015).
- [32] A. Fert, N. Reyren, and V. Cros, Nat. Rev. Mater. **2**, 17031 (2017).
- [33] A. F. Schaffer, L. Rozsa, J. Berakdar, E. Y. Vedmedenko, and R. Wiesendanger, Commun. Phys. **2**, 72 (2019).
- [34] M. Ezawa, Phys. Rev. B **83**, 100408(R) (2011).
- [35] X. Chen, W. Kang, D. Zhu, X. Zhang, N. Lei, Y. Zhang, Y. Zhou and W. Zhao, Nanoscale, 2018, **10**, 6139.
- [36] A. Bernard-Mantel, C. B. Muratov, and T. M. Simon, Phys. Rev. B **101**, 045416 (2020).
- [37] X. Chen, M. Lin, J. F. Kong, H. R. Tan, A. K. Tan, S. Je, H. K. Tan, K. H. Khoo, M. Im, and A. Soumyanarayanan, Advanced Science **9**, 2103978 (2022).
- [38] Here, it is worthwhile to point out that these solutions of the restricted gauged baby Skyrme model are not the magnetic skyrmions describing the material magnetization in condensed matter systems.
- [39] Here, for the $(1+2)$ -dimensional Minkowski space we adopt the metric with signature $(+, -, -)$. Moreover, we take the natural units $\hbar = c = 1$.
- [40] E. Witten and D. Olive, Phys. Lett. B **78**, 97 (1978).
- [41] Z. Hlousek and D. Spector, Nucl. Phys. B **370**, 143 (1992); **397**, 173 (1993).
- [42] M. Nitta, S. Sasaki, Phys. Rev. D **90**, 105001 (2014).

- [43] M.Nitta, S.Sasaki, Phys. Rev. D **91**, 125025 (2015).
- [44] Rodolfo Casana and André C. Santos, Phys. Rev. D **104**, 065009 (2021).
- [45] D. Bazeia, J. Menezes, and R. Menezes, Phys. Rev. Lett. **91** 241601 (2003).
- [46] D. Bazeia, M. M. Doria, and E. I. B. Rodrigues, Phys. Lett. A **380**, 1947 (2016).
- [47] D. Bazeia, J. G. G. S. Ramos, and E. I. B. Rodrigues, J. Magn. Magn. Mater. **423**, 411 (2017).
- [48] D. Bazeia and A. Mohammadi, Phys. Lett. B **779**, 420 (2018).
- [49] Z.-M. He, L. Wen, Y.-J. Wang, G. P. Chen, R.-B. Tan, C.-Q. Dai, and X.-F. Zhang, Phys. Rev. E **99**, 062216 (2019).
- [50] P.-H. Lu, X.-F. Zhang, and C.-Q. Dai, Front. Phys. **17**, 42501 (2022).
- [51] D. Bazeia, M. A. Liao, and M. A. Marques, Eur. Phys. J. Plus **135**, (2020) 383.
- [52] Y. V. Kartashov, V. A. Vysloukh, and L. Torner, Phys. Rev. Lett. **93**, 093904 (2004).
- [53] Y. V. Kartashov, V. A. Vysloukh, and L. Torner, Phys. Rev. Lett. **94**, 043902 (2005).
- [54] F. Hanada and N. Sawado, Nucl. Phys. B **996**, 116377 (2023).